Nanostructures

DOI: 10.1002/anie.201207909

Multifunctional Gold Nanorods with Ultrahigh Stability and Tunability for In Vivo Fluorescence Imaging, SERS Detection, and Photodynamic Therapy**

*Yuan Zhang, Jun Qian, Dan Wang, Yalun Wang, and Sailing He**

Along with the great development of nanotechnology, many kinds of colloidal nanoparticles have become powerful tools in various applications.[1] In recent years, focus has been put on the study of gold nanoparticles, because of their good properties, which are different from the traditional bulk materials.[2] Among them, gold nanorods (GNRs) have drawn more attention owing to their well-defined optical features, especially surface plasmon resonance (SPR), which makes them ideal enhancement agents.[3] One of the best developed GNR-assisted techniques is surface-enhanced Raman scattering (SERS),[4] through which a Raman signal can be enhanced dramatically with a factor of 10^9–10^{14}. This makes SERS a powerful tool both for biosensing[5] and imaging.[6] However, limited by the relatively weak signal intensity and the feature of the tools, SERS detection and imaging can only be realized by point-scan with long measuring time. In contrast, multiple kinds of imaging techniques based on GNRs have been well-developed, such as dark-field scattering imaging,[7] photoacoustic imaging,[8] and two-photon luminescence,[9] with fast or even real-time response.

It is known that the nanoparticles can be taken up by malignant tissues (e.g., tumors) through "enhanced permeability and retention" (EPR);[10] the utilization of such nanoparticles is therefore a promising tool in in vivo diagnostic or curing applications such as photodynamic therapy (PDT). PDT treatment requires a photosensitizer and light (at a proper wavelength) that can activate it. When irradiated by the light, the photosensitizer transfers the light energy to oxygen in tissue, thereby generating reactive oxygen species (ROS) in the form of free radicals or singlet oxygen,[11] which only kills the cells in the exposed area. Assisted by nanoparticles, the PDT photosensitizers can selectively accumulate in the tumor, thereby realizing targeted or even SPR-enhanced therapy.[12]

The multimodal utilization is one of the emerging developments related to nanomaterials and has been reported in some recent work.[13] Herein, a novel structure to achieve in vivo multimodal tumor detection is designed. SERS and fluorescence agents are chemically doped in different layers of a silica/polymer-coated GNR, thereby forming two individual "channels". By utilizing a chemical approach, the optical properties of the structure can be easily tuned. Its chemical and biological stability is also ultrahigh. After tuned to achieve satisfactory SERS and fluorescence intensities and intravenously injected into tumor-bearing mice, these nanoparticles can accumulate inside the tumors, thus allowing detection of the tumor by SERS and fluorescence measurements. Furthermore, through the same doping method, a PDT photosensitizer, protoporphyrin IX (PpIX), is also loaded into the multilayered shell, and PDT treatment is conducted right after the detection of the tumor. To our knowledge, this is the first report of tunable triple-modal functionality (integrated with PDT) with a GNR-based structure.

Gold nanorods were prepared by the seed-mediated method.[14] To synthesize the GNRs functionalized for both SERS and fluorescence measurements (abbreviation: SF-GNRs), the GNRs were capsulated sequentially by silica,[15] octadecyltrimethoxysilane (OTMS), and DSPE-PEG;[16] during the procedure dyes were doped in the silica shell and the polymer shell (Figure 1 a). Although the coating procedures of nondoped silica and PEG could be found in previous work, the addition of dyes made these procedures more difficult and thus required tuning the amounts of the reaction components as well as carefully controlling the time and speed of the centrifugation. For the sake of simplicity, in this paper, 3,3′-diethylthiatricarbocyanine iodide (DTTC) was used as dye in both silica and PEG. In most experiments, its 508 cm^{-1} SERS peak and fluorescence peak (about 780 nm) were measured as SERS and fluorescence intensities, respectively. By changing the concentration of the tetraethylorthosilicate (TEOS) when the silica shell is formed, the shell thickness of the SF-GNRs can be adjusted. According to the TEM images in Figure 1, the silica thickness (and the corresponding multilayer thickness) increases from less than 5 nm to more than 25 nm when the TEOS amount changes from 100 μL to 1100 μL in every 5 mL reaction solution.

According to previous research,[17] fluorescence quenching may occur owing to the relatively short distance between dye molecules and GNRs. Therefore the SERS and fluores-

[*] Y. Zhang, Dr. J. Qian, D. Wang, Y. Wang, Prof. S. He
Centre for Optical and Electromagnetic Research
Zhejiang Provincial Key Laboratory for Sensing Technologies
JORCEP [Joint Research Center of Photonics of the Royal Institute of Technology (Sweden), Lund University (Sweden), and Zhejiang University], Zhejiang University
Hangzhou, 310058 (China)
E-mail: sailing@kth.se

[**] This work was partially supported by the Science and Technology Department of Zhejiang Province, the National Basic Research Program (973) of China (2011CB503700), the National Natural Science Foundation of China (61008052 and 61108022), and the Fundamental Research Funds for the Central Universities. SERS = surface-enhanced Raman scattering.

Supporting information (including experimental details and other supplement experiments) for this article is available on the WWW under http://dx.doi.org/10.1002/anie.201207909.

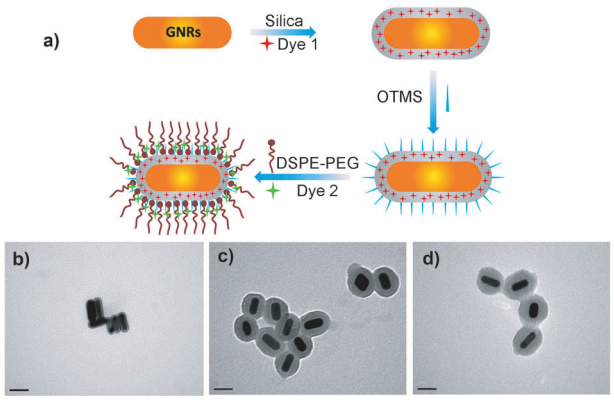

Figure 1. a) The synthesis procedures of the SF-GNRs; DSPE = 1,2-distearoyl-*sn*-glycero-3-phosphoethanolamine, PEG = poly(ethylene glycol). b–d) The TEM images when the tetraethylorthosilicate (TEOS) amount is 100 μL (b), 500 μL (c), and 1100 μL (d) in every 5 mL reaction solution. The length of the scale bar is 50 nm.

cence intensities of the SF-GNRs are closely related to the shell thickness, because it directly determines the average distance between dyes and GNRs. Figure 2 shows the connections between the optical properties of the SF-GNRs and the thickness. If more TEOS was added (i.e., if the silica shell became thicker), the SERS intensity experienced a sharp decline and finally disappeared, owing to the weaker SPR at a longer distance. There was an abrupt drop of the SERS intensity when the amount of TEOS was 50 μL, possibly caused by the decreasing dye loading capacity of the ultrathin silica shell. In contrast, the fluorescence signal gradually grew, mainly owing to the reduced quenching effect (see the Supporting Information for a schematic illustration). The distance-related intensity changes imply: 1) The SF-GNRs can be easily tuned to be only functionalized for SERS, or only functionalized for fluorescence, or functionalized for both SERS and fluorescence measurements; 2) owing to the different distances from the GNR, dye1 and dye2 have a higher efficiency for SERS and fluorescence, respectively, so the "SERS channel" and the "fluorescence channel" in this structure are separated. Another method to control the optical properties is to change the types of dyes (see Figure S5 in the Supporting Information). These features make SF-GNRs a powerful tool in applications with various requirements.

Some previous work has shown that the multilayered GNR structures are super-stable in various solutions like NaCl, phosphate-buffered saline (PBS), RPMI culture medium, etc., although this high stability has not been completely understood.[18] The stability testing in water solution at different pH values is very essential for our research, since 1) most biological reactions are performed between pH 4–8, and the pH values of creatures are also in this range; 2) so far there is no report on the investigation of the pH stability of the silica/polymer-coated GNRs; 3) dye-induced effects are unknown, which might be a negative factor for the shell protection. Furthermore, given that our structure is aimed to be used inside a living body, its stability in animal serum should also be tested. To check the stabilities of the SF-GNRs as well as each of its "channels", three types of structures were dispersed in water solutions with pH values between 1 and 12 as well as in serum: S-GNRs (only dye1 was doped), F-GNRs (only dye2 was doped), and SF-GNRs. The TEOS concentrations of all the GNRs were 100 μL in every 5 mL reaction solution. After 24 h, their SERS and/or fluorescence intensities were measured (Figure 3). The intensities of the three kinds of GNRs have similar variation tendencies. Both SERS and fluorescence signals obviously increased when pH > 9; this might be caused by the plasmon "hot-spots" in the slight aggregation of GNRs owing to the partial degradation of the silica shell. In contrast, because of the imperfect packaging of the dye molecules in the multilayered shell and the nonideal stability of DTTC in the solution, when pH < 5, SERS and fluorescence intensities

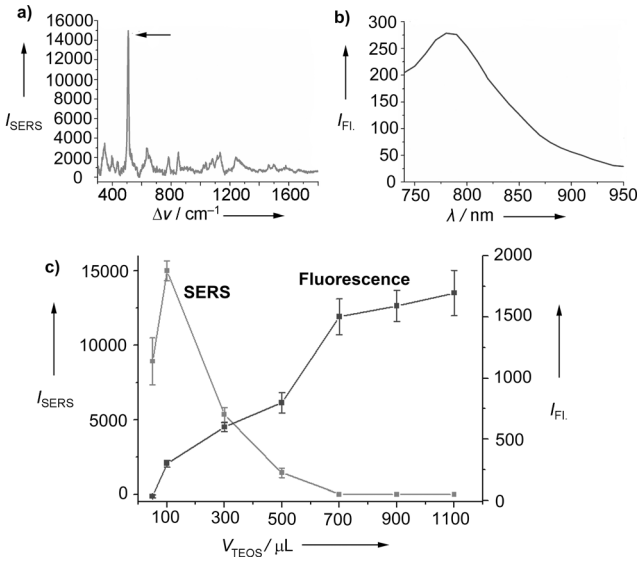

Figure 2. a) The SERS and b) the fluorescence spectrum of DTTC. c) The variation of SERS and fluorescence when different amounts of TEOS were added (which corresponds to the increasing shell thickness). The 508 cm^{-1} SERS peak (pointed by the arrow) and the fluorescence peak (at about 780 nm) were chosen as the SERS and fluorescence intensities in (c), respectively.

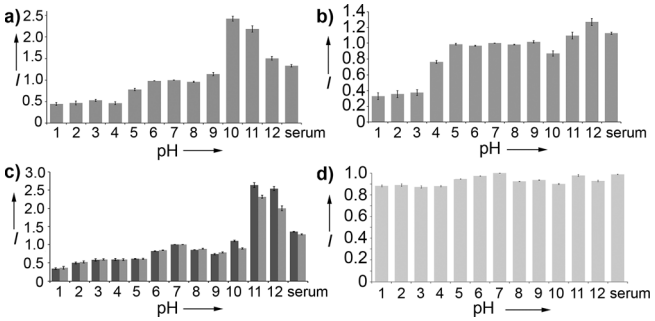

Figure 3. The variation of signal intensities in water solutions with different pH values and in serum: a) SERS of S-GNRs; b) fluorescence of F-GNRs; c) SERS (dark-gray bars) and fluorescence (light-gray bars) of SF-GNRs; d) absorption intensity at the longitudinal SPR wavelength of the SF-GNRs, measured 24 h after the dispersion.

decreased to 1/3 but were still large enough to be detected. In the meantime, the optical properties of all the GNRs in serum were maintained. We also measured the absorption spectra of the SF-GNRs and found that the absorption intensities of the GNRs in all these solutions remained nearly the same (Figure 3d), indicating no severe destruction of the multi-shell occurred. The results verify that the SF-GNRs have an extraordinary structural stability in acids, bases, and animal serum, and the SERS and fluorescence intensities were also stable in these solutions. Besides, we observed the distribution, circulation, and excretion of the intravenously injected SF-GNRs inside mice bodies and found their optical properties could be maintained for more than 72 h, ensuring its excellent stability in vivo (see Figure S6 in the Supporting Information).

For in vivo tumor detection, in a typical experiment, the SF-GNRs (with the TEOS concentration of 200 μL in every 5 mL reaction solution) in PBS buffer solution (1X) were intravenously injected into a nude mouse bearing HeLa tumor (Figure 4a). Five hours after the injection, the mouse was imaged by a Maestro fluorescence imaging system, and a fluorescence image was obtained automatically in less than three minutes, in which three locations with relatively strong signals were observed (pointed by arrows in Figure 4b). The fluorescence spectra were recorded (Figure 4c). Only the spectrum from location 1 (the tumor) was the same as that of DTTC, while the peaks of the spectra from the other two positions were both at a shorter wavelength. This difference indicated that only location 1 should be the accumulation area of the GNRs and that the strong signals from locations 2 and 3 were probably from the tissues or some metabolic organs (such as liver and kidney). These "false-positive" signals appeared possibly owing to the spectra separation algorithm of the equipment. The SERS measurements were also carried out at the three locations to confirm the accumulation because it requires the presence of both GNRs and DTTC. A very intense SERS signal was observed at location 1 (Figure 4d), thereby revealing the accumulation of GNRs at that area, which was in accord with the fluorescence imaging. This dual-modal detection combines the advantages of the two methods, and their weaknesses could be compensated by each other: the fluorescence imaging offers a fast and wide-area detection to quickly find the "suspicious" spots, and the specific and high-contrast SERS measurement directly confirms the actual location of the GNRs.

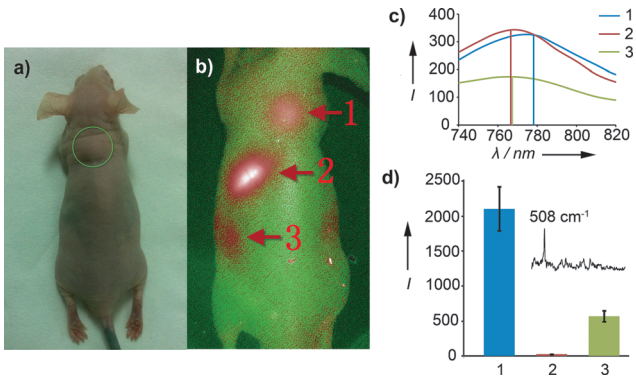

Figure 4. a) The photo of the mouse bearing a tumor (green circle). b) Fluorescence image with three locations emitting strong signals (red arrows). c) The fluorescence spectra and d) the 508 cm^{-1} SERS intensities from the three locations. The inset in (d) shows an SERS trace.

In SF-GNRs, dyes were doped in the pores and spaces in the multilayered shell. Similarly, PDT photosensitizers could also be loaded by adding some PpIX when DTTC was doped, forming multifunctionalized GNRs (SFP-GNRs) for SERS and fluorescence measurements as well as PDT treatment. The successful loading was proved through the chemical oxidation of 1,3-diphenylisobenzofuran (DPBF; Figure S8 in the Supporting Information).[19] An in vitro experiment was carried out to verify the PDT effect to the tumor cells (Figure S9 in the Supporting Information). To confirm that the EPR effect of GNRs was still maintained after the doping of PpIX, and that the GNRs were inside the tumor rather than at the surrounding skins, the tumor-bearing mice were sacrificed five hours after the intravenous injection of SFP-GNRs. The tumors were removed and cut from their middle, and the SERS measurements were conducted on the cut surfaces. The accumulation of the GNRs was proved by the SERS signals from inside the tumors (Figure S10 in the Supporting Information).

For the in vivo PDT treating, the SFP-GNRs were intravenously injected into the tumor-bearing mice. Five hours after the injection, the tumors were exposed to a 532 nm laser for 15 min at a power density of about 25 mW cm^{-2}, with 1 min interval for every 1 min treatment. Hematoxylin and eosin (H&E)-stained tumor slices obtained seven days after the treatment were used to evaluate the treating effect. A large area of dead cells without nuclei could be clearly seen in the PDT-treated tumors (Figure 5a), while many nuclei existed in the control groups that lack of either laser irradiation (Figure 5b) or SFP-GNRs (Figure 5c). Furthermore, there was also no obvious damage in tumors treated by both SF-GNRs injection and laser irradiation (Figure 5d), thus indicating the destruction was due to the singlet oxygen produced by PpIX rather than the photothermal effect of GNRs.[20] The tumor cell death rates of the above groups (Figure 5e) show that a larger percentage of dead cells existed in the PDT-treated tumors, thereby revealing more serious

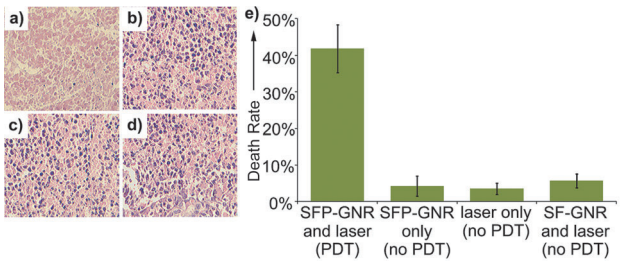

Figure 5. H&E-stained tumor slices after different treating: a) SFP-GNR injection and laser (PDT), b) SFP-GNRs injection only, c) laser only, d) SF-GNR injection and laser. e) Tumor cell death rate of the above groups. In (a–d) the blue dots indicate the cell nuclei.

necrosis inside them. This experiment is a proof of the potential use of our multifunctional GNRs in drug-delivery and PDT treatment.

In conclusion, we have demonstrated a multilayer-coated GNR, which contained dyes doped in silica and polymer layers, functioning as SERS channel and fluorescence channel, respectively. Its optical properties could be easily tuned, by either adjusting the shell thickness or changing the type of the dyes in each layer. The GNRs have been shown to be ultrastable in water solutions with pH values between 1 and 12, in animal serum, and in living systems. The potentials of such GNRs in simultaneous multimodal tumor detection and photodynamic therapy have also been shown.

Received: October 1, 2012
Published online: December 11, 2012

Keywords: fluorescence · gold · imaging agents · photodynamic therapy · surface-enhanced Raman scattering

[1] a) W. S. Kuo, C. N. Chang, Y. T. Chang, M. H. Yang, Y. H. Chien, S. J. Chen, C. S. Yeh, *Angew. Chem.* **2010**, *122*, 2771; *Angew. Chem. Int. Ed.* **2010**, *49*, 2711; b) Q. Q. Zhan, J. Qian, H. J. Liang, G. Somesfalean, D. Wang, S. L. He, Z. G. Zhang, S. Andersson-Engels, *ACS Nano* **2011**, *5*, 3744; c) R. Bukasov, J. S. Shumaker-Parry, *Anal. Chem.* **2009**, *81*, 4531.

[2] J. Pérez-Juste, I. Pastoriza-Santos, L. M. Liz-Marzán, P. Mulvaney, *Coord. Chem. Rev.* **2005**, *249*, 1870.

[3] a) E. B. Dickerson, E. C. Dreaden, X. H. Huang, I. H. El-Sayed, H. H. Chu, S. Pushpanketh, J. F. McDonald, M. A. El-Sayed, *Cancer Lett.* **2008**, *269*, 57; b) T. S. Troutman, J. K. Barton, M. Romanowski, *Opt. Lett.* **2007**, *32*, 1438.

[4] a) C. V. Raman, K. S. Krishnan, *Indian J. Phys.* **1928**, *2*, 399; b) C. V. Raman, K. S. Krishnan, *Nature* **1928**, *121*, 501.

[5] Y. C. Cao, R. C. Jin, C. A. Mirkin, *Science* **2002**, *297*, 1536.

[6] G. L. Liu, Y. Lu, J. Kim, J. C. Doll, L. P. Lee, *Adv. Mater.* **2005**, *17*, 2683.

[7] X. H. Huang, I. H. El-Sayed, W. Qian, M. A. El-Sayed, *J. Am. Chem. Soc.* **2006**, *128*, 2115.

[8] M. Eghtedari, A. Oraevsky, J. A. Copland, N. A. Kotov, A. Conjusteau, M. Motamedi, *Nano Lett.* **2007**, *7*, 1914.

[9] H. F. Wang, T. B. Huff, D. A. Zweifel, W. He, P. S. Low, A. Wei, J. X. Cheng, *Proc. Natl. Acad. Sci. USA* **2005**, *102*, 15752.

[10] H. Maeda, J. Wu, T. Sawa, Y. Matsumura, K. Hori, *J. Controlled Release* **2000**, *65*, 271.

[11] B. W. Henderson, T. J. Dougherty, *Photochem. Photobiol.* **1992**, *55*, 145.

[12] a) J. Qian, D. Wang, F. H. Cai, Q. Q. Zhan, Y. L. Wang, S. L. He, *Biomaterials* **2012**, *33*, 4851; b) M. Olivo, R. Bhuvaneswari, S. S. Lucky, N. Dendukuri, P. S. Thong, *Pharmaceuticals* **2010**, *3*, 1507; c) M. K. K. Oo, Y. Yang, Y. Hu, M. Gomez, H. Du, H. Wang, *ACS Nano* **2012**, *6*, 1939.

[13] a) Y. I. Park, H. M. Kim, J. H. Kim, K. C. Moon, B. Yoo, K. T. Lee, N. Lee, Y. Choi, W. Park, D. Ling, K. Na, W. K. Moon, S. H. Choi, H. S. Park, S. Yoon, Y. D. Suh, S. H. Lee, T. Hyeon, *Adv. Mater.* **2012**, *24*, 5755; b) M. F. Kircher, A. de La Zerda, J. V. Jokerst, C. L. Zavaleta, P. J. Kempen, E. Mittra, K. Pitter, R. Huang, C. Campos, F. Habte, R. Sinclair, C. W. Brennan, I. K. Mellinghoff, E. C. Holland, S. S. Gambhir, *Nat. Med.* **2012**, *18*, 829.

[14] J. Pérez-Juste, L. M. Liz-Marzán, S. Carnie, D. Y. C. Chan, P. Mulvaney, *Adv. Funct. Mater.* **2004**, *14*, 571.

[15] Q. Q. Zhan, J. Qian, X. Li, S. L. He, *Nanotechnology* **2010**, *21*, 055704.

[16] X. G. Hu, X. H. Gao, *Phys. Chem. Chem. Phys.* **2011**, *13*, 10028.

[17] a) X. Li, J. Qian, L. Jiang, S. L. He, *Appl. Phys. Lett.* **2009**, *94*, 063111; b) G. Schneider, G. Decher, N. Nerambourg, R. Praho, M. H. V. Werts, M. Blanchard-Desce, *Nano Lett.* **2006**, *6*, 530.

[18] X. G. Hu, X. H. Gao, *ACS Nano* **2010**, *4*, 6080.

[19] W. Spiller, H. Kliesch, D. Wöhrle, S. Hackbarth, B. Röder, G. J. Schnurpfeil, *J. Porphyrins Phthalocyanines* **1998**, *2*, 145.

[20] R. Weissleder, *Nat. Biotechnol.* **2001**, *19*, 316.

